Homogeneous dynamic characteristics of damped 2D elastic lattices

Sondipon Adhikari

Zienkiewicz Centre for Computational Engineering, College of Engineering, Swansea University, Bay Campus, Swansea, Wales, UK, Email: S.Adhikari@swansea.ac.uk
Twitter: @ProfAdhikari, Web: http://engweb.swan.ac.uk/~adhikaris

1st International Conference on Recent Advances in Computational and Experimental Mechanics (ICRACEM 2020), IIT Kharagpur, 5 September 2020

Outline

- **Dr T. Mukhopadhyay**, Department of Aerospace Engineering, Indian Institute of Technology Kanpur, Kanpur, India.
- **Dr X. Liu**, Key Laboratory of Traffic Safety on Track, Ministry of Education, School of Traffic & Transportation Engineering, Central South University, Changsha, China.
- **Dr A. Shaw**, Zienkiewicz Centre for Computational Engineering, College of Engineering, Swansea University, Bay Campus, Swansea, Wales, UK.
- **Dr N. Levery**, Future Manufacturing Research Institute, College of Engineering, Swansea University, Bay Campus, Swansea, Wales, UK.

Metamaterials

- Metamaterials are designer media with periodic units comprised of unique tailor-made geometry and pattern aimed at accomplishing exceptional and unusual bulk properties which are unprecedented in conventional materials.
- Mechanical metamaterials achieve their unusual effective properties from the geometry and structure, and not from the intrinsic property of the constitutive material.
- An essential feature of metamaterials, operating in any frequency ranges or of any length-scales, is the periodicity of a unit cell:
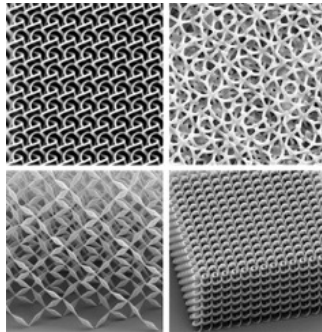
- In 1898, **Jagadish Chandra Bose** conducted the first microwave experiment on twisted structures. These twisted structures match the geometries that are known as artificial chiral media in today's terminology. He also researched double refraction (birefringence) in crystals. Other research included polarization of electric field "waves" that crystals produce. He discovered this type of polarization in other materials including a class of dielectrics.

- The origin of modern metamaterials was in field of *electromagnetism* and ideas can be traced back to 1967 from Russia.

- However, it was the seminal paper by Smith et al. in 2000 demonstrating negative permeability and permittivity by a periodic array of split-ring resonators, that started the current interest in metamaterials.

- Since then several concepts and devices have been conceived which challenge conventional physical laws, such as negative refraction, the perfect lens, and invisibility cloaking in electromagnetism and optics.

- These extraordinary developments not only attracted researchers but also captured the imagination of the public and in some cases, science fiction.

- The next round of development was in *acoustic* metamaterials exploiting the idea of locally resonant behaviour.

- The consideration of sub-wavelength structures opened up immense possibilities, including negative effective elastic modulus, negative density (or mass), or both, anisotropy in the effective mass or density and non-reciprocal response.

- The *mechanical* metamaterials emerged following in the footsteps of electromagnetic and acoustic metamaterials, primarily within the past 10 years.

- Intense research in recent years shows ultralight metamaterials approaching theoretical strength limit, pentamode materials with cloaking mode, negative refraction elastic waves, elastic cloaking and hyperbolic elastic metamaterials.

- The rise of mechanical metamaterials coincides with remarkable recent advances in manufacturing technology and 3D printing.
- From the point of view of analytical techniques, two distinct type of metamaterials are considered, namely, (1) static mechanical metamaterials and (2) dynamic mechanical metamaterials.
- The roots of static mechanical metamaterials can be traced back to late 80's with the discovery of negative Poisson's ratio cellular structures.
- Dynamic metamaterials differ from static metamaterials by a crucial point - it is the dynamic metamaterials which explicitly exploits sub-wavelength scale properties.
- This talk is related to dynamic behaviour of cellular metamaterials.
- The dynamic behaviour makes the equivalent in-plane properties frequency dependent.

- **Lattice** based metamaterials are abundant in man-made and natural systems at various length scales.
- They are made of **periodic** identical/near-identical geometric units.
- Among various lattice geometries (triangle, square, rectangle, pentagon, hexagon), **hexagonal lattice** is most common (note that hexagon is the highest "space filling" pattern in 2D).
- This talk is about **in-plane** viscoelastic properties of 2D hexagonal lattice structures - commonly known as "honeycombs"

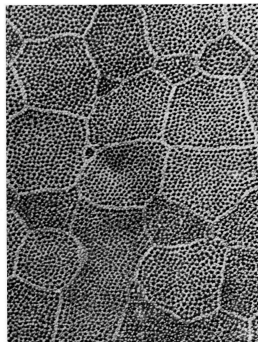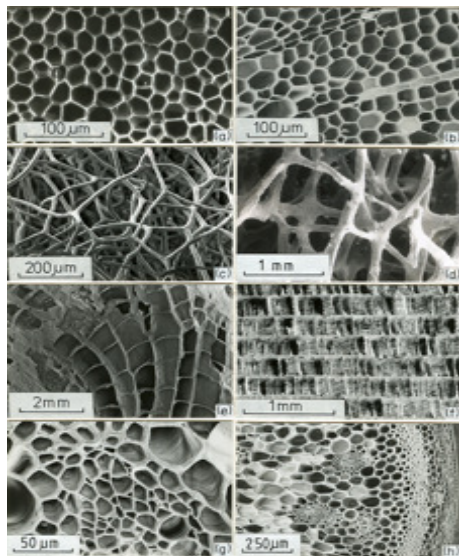

www.shutterstock.com · 113350987
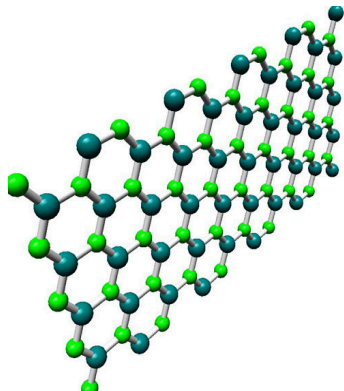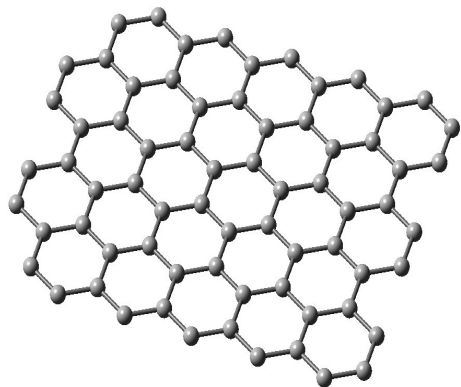
Illustrations of a single layer graphene sheet and a born nitride nano sheet
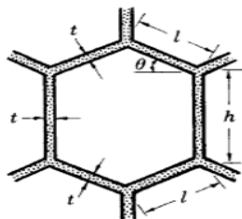
Lattice structures - nature

Top left: cork, top right: balsa, next down left: sponge, next down right: trabecular bone, next down left: coral, next down right: cuttlefish bone, bottom left: leaf tissue, bottom right: plant stem, third column - epidermal cells (from web.mit.edu)

- Hexagonal lattice structures have been modelled as a continuous solid with an equivalent elastic moduli throughout its domain.
- This approach eliminates the need of detail finite element modelling of lattices in complex structural systems like sandwich structures.
- Extensive amount of research has been carried out to predict the equivalent elastic / viscoelastic properties of regular lattices consisting of perfectly periodic hexagonal cells.
- Analysis of two dimensional hexagonal lattices dealing with in-plane elastic properties are commonly based on an unit cell approach, which is applicable only for perfectly periodic cellular structures.
- For the dynamic analysis of perfectly periodic structures, Floquet-Bloch theorem is normally employed to characterise wave propagation.

- Unit cell approach - Gibson and Ashby (1999)
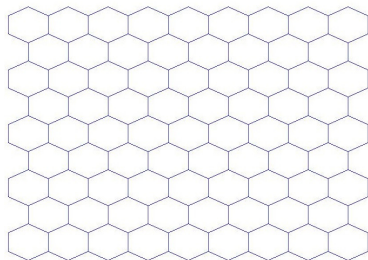
(a) Regular hexagon ($\theta = 30°$)   (b) Unit cell

- We are interested in homogenised equivalent in-plane elastic properties
- This way, we can avoid a detailed structural analysis considering all the beams and treat it as a material

- The cell walls are treated as beams of thickness t, depth b and Young's modulus E_s. l and h are the lengths of inclined cell walls having inclination angle θ and the vertical cell walls respectively.

- The equivalent elastic properties are:

$$E_1 = E_s \left(\frac{t}{l}\right)^3 \frac{\cos\theta}{\left(\frac{h}{l} + \sin\theta\right)\sin^2\theta} \tag{1}$$

$$E_2 = E_s \left(\frac{t}{l}\right)^3 \frac{\left(\frac{h}{l} + \sin\theta\right)}{\cos^3\theta} \tag{2}$$

$$\nu_{12} = \frac{\cos^2\theta}{\left(\frac{h}{l} + \sin\theta\right)\sin\theta} \tag{3}$$

$$\nu_{21} = \frac{\left(\frac{h}{l} + \sin\theta\right)\sin\theta}{\cos^2\theta} \tag{4}$$

$$G_{12} = E_s \left(\frac{t}{l}\right)^3 \frac{\left(\frac{h}{l} + \sin\theta\right)}{\left(\frac{h}{l}\right)^2 \left(1 + 2\frac{h}{l}\right)\cos\theta} \tag{5}$$

- A finite element code has been developed to obtain the in-plane elastic moduli numerically for hexagonal lattices.
- Each cell wall has been modelled as an Euler-Bernoulli beam element having three degrees of freedom at each node.
- For E_1 and ν_{12}: two opposite edges parallel to direction-2 of the entire hexagonal lattice structure are considered. Along one of these two edges, uniform stress parallel to direction-1 is applied while the opposite edge is restrained against translation in direction-1. Remaining two edges (parallel to direction-1) are kept free.
- For E_2 and ν_{21}: two opposite edges parallel to direction-1 of the entire hexagonal lattice structure are considered. Along one of these two edges, uniform stress parallel to direction-2 is applied while the opposite edge is restrained against translation in direction-2. Remaining two edges (parallel to direction-2) are kept free.
- For G_{12}: uniform shear stress is applied along one edge keeping the opposite edge restrained against translation in direction-1 and 2, while the remaining two edges are kept free.
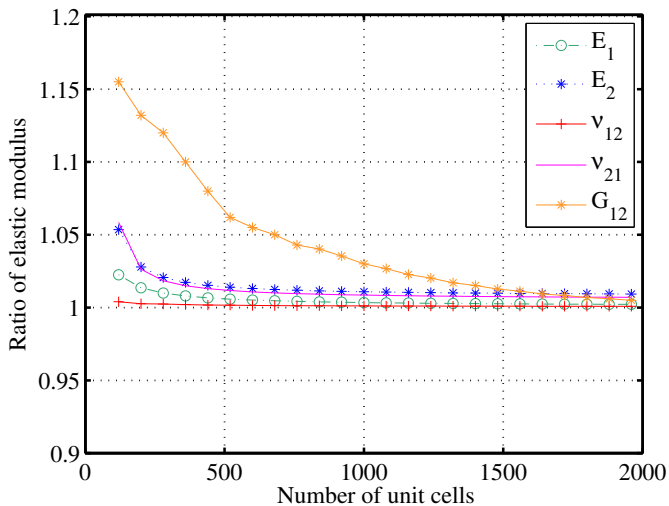
$\theta = 30°$, $h/l = 1.5$. FE results converge to analytical predictions after 1681 cells.

- How can we obtain such equivalent homogenised properties when the lattices behave in a dynamic manner?
- What role the mass density and damping play for the dynamic case?
- How the elastic moduli and Poisson's ratio would change as functions of frequency?
- Is it possible to have closed-form expressions similar to the classical static homogeneous properties?
- Does the consideration of dynamic behaviour unlock any new physics which is not present in the static case?
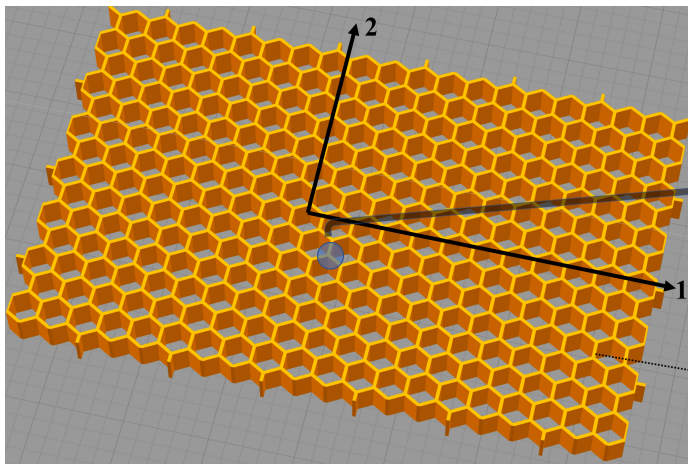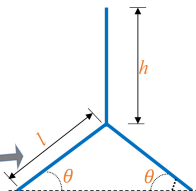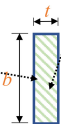
(a) Typical representation of a hexagonal lattice (b) The unit cell considered in this paper. Dimensions of the three-beam element are shown in the figure (c) The out of plane cross-section of each beam element.
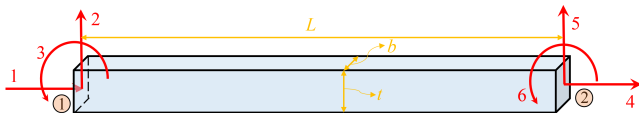
- A beam element with six degrees of freedom and two nodes is shown. The degrees of freedom in each node corresponds to the axial, transverse and rotational deformation.

- The static stiffness matrix using the Euler-Bernoulli beam theory is given by

$$
\mathbf{K}_s = \begin{bmatrix}
\frac{EA}{L} & 0 & 0 & -\frac{EA}{L} & 0 & 0 \\
0 & \frac{12EI}{L^3} & \frac{6EI}{L^2} & 0 & -\frac{12EI}{L^3} & \frac{6EI}{L^2} \\
0 & \frac{6EI}{L^2} & \frac{4EI}{L} & 0 & -\frac{6EI}{L^2} & \frac{2EI}{L} \\
-\frac{EA}{L} & 0 & 0 & \frac{EA}{L} & 0 & 0 \\
0 & -\frac{12EI}{L^3} & -\frac{6EI}{L^2} & 0 & \frac{12EI}{L^3} & -\frac{6EI}{L^2} \\
0 & \frac{6EI}{L^2} & \frac{2EI}{L} & 0 & -\frac{6EI}{L^2} & \frac{4EI}{L}
\end{bmatrix}
\tag{6}
$$

Dynamic stiffness of a beam

- The mass distribution of the element is treated in an exact manner in deriving the element dynamic stiffness matrix.
- The dynamic stiffness matrix of one-dimensional structural elements, taking into account the effects of flexure, torsion, axial and shear deformation, and damping, is exactly determinable, which, in turn, enables the exact vibration analysis by an inversion of the global dynamic stiffness matrix.
- The method does not employ eigenfunction expansions and, consequently, a major step of the traditional finite element analysis, namely, the determination of natural frequencies and mode shapes, is eliminated which automatically avoids the errors due to series truncation.
- The damping within the system can be incorporated in a rigorous manner using complex algebra.
- The method is essentially a frequency-domain approach suitable for steady state harmonic or stationary random excitation problems.
- The static stiffness matrix and the consistent mass matrix appear as the first two terms in the Taylor expansion of the dynamic stiffness matrix in the frequency parameter.

- The equation governing axial motion of a beam is

$$EA\left(1 + \zeta_k\frac{\partial}{\partial t}\right)\frac{\partial^2 u}{\partial x^2} - \rho A\frac{\partial^2 u}{\partial t^2} - c_a\frac{\partial u}{\partial t} = 0 \tag{7}$$

and the axial force boundary condition is

$$N(x) = EA\left(1 + \zeta_k\partial/\partial t\right)\partial u/\partial x \tag{8}$$

- Here EA is the stiffness for axial deformation, ρA is mass per unit length, ζ_k is the stiffness proportional damping factor, c_a is the velocity-dependent viscous damping coefficient.

- By introducing the non-dimensional length $\xi = x/L$ and harmonic vibration assumption $u(x,t) = U(x)e^{i\omega t}$, one has the characteristic equation

$$\frac{\mathrm{d}^2 U}{\mathrm{d}\xi^2} + k_a^2 U = 0 \tag{9}$$

where

$$k_a^2 = \frac{\left(\rho A\omega^2 - i\omega c_a\right)L^2}{EA\left(1 + i\omega\zeta_k\right)} = \frac{m\omega^2 L^2\left(1 - i\zeta_{ma}/\omega\right)}{E\left(1 + i\omega\zeta_k\right)} \tag{10}$$

and $\zeta_{ma} = c_a/(\rho A)$ is the mass proportional damping factor.

- The exact shape function can be derived

$$U(\xi) = c_1 \cos\left(k_a \xi\right) + c_2 \sin\left(k_a \xi\right) \tag{11}$$

- Therefore, the displacement boundary conditions for a beam element can be written in the matrix form as

$$\left[\begin{array}{c} U_1 \\ U_2 \end{array}\right] = \left[\begin{array}{c} U(\xi = 0) \\ U(\xi = 1) \end{array}\right] = \left[\begin{array}{cc} 1 & 0 \\ \cos\left(k_a\right) & \sin\left(k_a\right) \end{array}\right] \left[\begin{array}{c} c_1 \\ c_2 \end{array}\right] \tag{12}$$

whereas the force boundary conditions can be given as

$$\left[\begin{array}{c} N_1 \\ N_2 \end{array}\right] = \left[\begin{array}{c} -N(\xi = 0) \\ N(\xi = 1) \end{array}\right] =$$
$$\frac{EA\left(1 + i\omega\zeta_k\right) k_a}{L} \left[\begin{array}{cc} 0 & -1 \\ -\sin\left(k_a\right) & \cos\left(k_a\right) \end{array}\right] \left[\begin{array}{c} c_1 \\ c_2 \end{array}\right] \tag{13}$$

- Eliminating the unknowns c_1, c_2 leads to the dynamic stiffness formulation for the axial vibration of a beam element

$$\begin{bmatrix} N_1 \\ N_2 \end{bmatrix} = \underbrace{\begin{bmatrix} a_1 & a_2 \\ a_2 & a_1 \end{bmatrix}}_{\mathbf{K}_a(\omega)} \begin{bmatrix} U_1 \\ U_2 \end{bmatrix} \tag{14}$$

where

$$a_1 = EA(1 + i\omega\zeta_k)\, k_a \cot(k_a)/L \tag{15}$$

$$a_2 = -EA(1 + i\omega\zeta_k)\, k_a \csc(k_a)/L. \tag{16}$$

- The governing differential equation for bending vibration based on Euler-Bernoulli beam theory is given as follows

$$EI\left(1 + \zeta_k \frac{\partial}{\partial t}\right)\frac{\partial^4 w}{\partial x^4} + \rho A \frac{\partial^2 w}{\partial t^2} + c_b \frac{\partial w}{\partial t} = 0 \qquad (17)$$

- The natural boundary conditions are given as

$$M(x) = EI\left(1 + \zeta_k \frac{\partial}{\partial t}\right)\frac{\partial^2 w}{\partial x^2}$$
$$V(x) = -EI\left(1 + \zeta_k \frac{\partial}{\partial t}\right)\frac{\partial^3 w}{\partial x^3} \qquad (18)$$

where c_b is the velocity-dependent viscous damping coefficient for bending deformation, EI is the bending stiffness of the beam, I is the inertia moment of the beam cross section.

- By introducing the harmonic vibration assumption $w(x, t) = W(x)e^{i\omega t}$, we have the following characteristic equation

$$\left(D^4 - k_b^4\right) W = 0 \tag{19}$$

where $D = d/d\xi = L d/dx$ and

$$k_b^4 = \frac{\left(\rho A \omega^2 - i\omega c_b\right) L^4}{EI\left(1 + i\omega\zeta_k\right)} = \frac{\rho A \omega^2 L^4 \left(1 - i\zeta_{mb}/\omega\right)}{EI\left(1 + i\omega\zeta_k\right)} = \frac{12\rho\omega^2 L^4 \left(1 - i\zeta_{mb}/\omega\right)}{Et^2\left(1 + i\omega\zeta_k\right)} \tag{20}$$

- Therefore, the general solutions are of the form

$$W(\xi) = c_1 \sin\left(k_b\xi\right) + c_2 \cos\left(k_b\xi\right) + c_3 \sinh\left(k_b\xi\right) + c_4 \cosh\left(k_b\xi\right)$$
$$\Theta(\xi) = c_1 k_b \cos\left(k_b\xi\right) - c_2 k_b \sin\left(k_b\xi\right) + c_3 k_b \cosh\left(k_b\xi\right) + c_4 k_b \sinh\left(k_b\xi\right) \tag{21}$$

- By eliminating the unknowns c_1, c_2, c_3 and c_4, we have the dynamic stiffness matrix for a Euler-Bernoulli beam element

$$
\begin{bmatrix} V_1 \\ M_1 \\ V_2 \\ M_2 \end{bmatrix} = \underbrace{\begin{bmatrix} d_1 & d_2 & d_4 & d_5 \\ & d_3 & -d_5 & d_6 \\ & & d_1 & -d_2 \\ sym & & & d_3 \end{bmatrix}}_{\mathbf{K}_b(\omega)} \begin{bmatrix} W_1 \\ \Theta_1 \\ W_2 \\ \Theta_2 \end{bmatrix} \tag{22}
$$

- Here the complex frequency-dependent functions

$$
\begin{aligned}
d_1 &= R_3 \left(cS + sC \right) / \delta \\
d_2 &= R_2 sS / \delta \\
d_3 &= R_1 \left(sC - cS \right) / \delta \\
d_4 &= -R_3 \left(s + S \right) / \delta \\
d_5 &= R_2 \left(C - c \right) / \delta \\
d_6 &= R_1 \left(S - s \right) / \delta
\end{aligned} \tag{23}
$$

and

$$
\begin{aligned}
\delta &= 1 - cC, \quad R_j = EI \left(k_b/L \right)^j \quad j = 1, 2, 3 \\
s &= \sin k_b, \quad c = \cos k_b, \quad S = \sinh k_b, \quad C = \cosh k_b
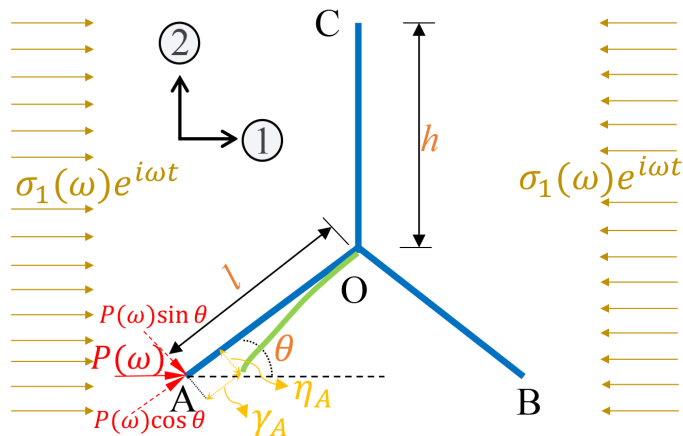\end{aligned} \tag{24}
$$

- Combining the axial and bending vibration cases, the elemental matrix of a beam element can be written as

$$\mathbf{K}(\omega) = \begin{bmatrix} a_1 & 0 & 0 & a_2 & 0 & 0 \\ 0 & d_1 & d_2 & 0 & d_4 & d_5 \\ 0 & d_2 & d_3 & 0 & -d_5 & d_6 \\ a_2 & 0 & 0 & a_1 & 0 & 0 \\ 0 & d_4 & -d_5 & 0 & d_1 & -d_2 \\ 0 & d_5 & d_6 & 0 & -d_2 & d_3 \end{bmatrix} \tag{25}$$

- The above equation is obtained using the shape functions exactly satisfying the equation of dynamic motion.
- All the non-zero elements are function of frequency and complex values due to the presence of damping.

- Dynamic behaviour of the overall lattice structure depends on the frequency-dependent deformation characteristics of the constituent individual beams.

- The vibrating beams undergo deformation under applied external harmonic loads. The rule of deformation in such cases would be different from the static condition.

- It will be shown that this leads to a different value of effective elastic moduli of the lattice material from conventional static values.

- Our objective is to express equivalent in-plane elastic moduli of the lattice in terms of the stiffness matrix elements of the beams using the unit cell approach.

- For the sake of generality, we consider the dynamic equilibrium of the unit cell under different stress conditions. The general frequency-dependent stiffness matrix $\mathbf{K}(\omega)$ derived before is employed here.

- Dynamic equilibrium and deformation patterns of the unit cell under the application of a harmonic stress field $\bar{\sigma}_1 = \sigma_1(\omega)e^{i\omega t}$ applied in the 1-direction. This configuration is used for the derivation of the longitudinal Young's modulus $E_1(\omega)$ and the Poisson's ratio $\nu_{12}(\omega)$.

- The deformation of the unit cell is symmetric about the OC line. The amplitude of the force P acting on point A for a given frequency ω is given by

$$P(\omega) = \sigma_1(\omega)b(h + l\sin\theta) \tag{26}$$

- Considering $\eta_A(\omega)$ and $\gamma_A(\omega)$ as deformations transverse and along the inclined member AO, we have

$$\eta_A(\omega) = \frac{P(\omega)\sin\theta}{K_{55}(\omega)} \quad \text{and} \quad \gamma_A(\omega) = \frac{P(\omega)\cos\theta}{K_{66}(\omega)} \tag{27}$$

- Here $K_{55}(\omega)$ and $K_{66}(\omega)$ are elements of the stiffness matrix of the inclined member AO of length l. Due to the presence of damping, $K_{55}(\omega)$ and $K_{66}(\omega)$ are in general complex valued functions of the frequency parameter ω. As a result, the deformations $\eta_A(\omega)$ and $\gamma_A(\omega)$ are complex valued functions of ω.

- The total dynamic deflection in the 1-direction is therefore

$$
\begin{aligned}
\delta_1(\omega) &= \eta_A(\omega)\sin\theta + \gamma_A(\omega)\cos\theta = P(\omega)\left(\frac{\sin^2\theta}{K_{55}(\omega)} + \frac{\cos^2\theta}{K_{66}(\omega)}\right) \\
&= \frac{P\sin^2\theta}{K_{55}(\omega)}\left(1 + \cot^2\theta\frac{K_{55}(\omega)}{K_{66}(\omega)}\right)
\end{aligned}
\tag{28}
$$

- The strain the 1-direction is obtained as

$$
\epsilon_1(\omega) = \frac{\delta_1(\omega)}{l\cos\theta} = \frac{\sigma_1(\omega)b(h/l + \sin\theta)\sin^2\theta}{K_{55}(\omega)\cos\theta}\left(1 + \cot^2\theta\frac{K_{55}(\omega)}{K_{66}(\omega)}\right)
\tag{29}
$$

- Using this, the Young's modulus in 1-direction is obtained in terms of the elements of the stiffness matrix as

$$
E_1(\omega) = \frac{\sigma_1(\omega)}{\epsilon_1(\omega)} = \frac{K_{55}(\omega)\cos\theta}{b(h/l + \sin\theta)\sin^2\theta\left(1 + \cot^2\theta\frac{K_{55}(\omega)}{K_{66}(\omega)}\right)}
\tag{30}
$$

- To obtain the Poisson's ratio ν_{12}, we need to obtain the strain in the direction 2 for applied stress in the 1-direction. Using the expressions of the deformations in Eq. (27), we obtain total deflection in the 2-direction as
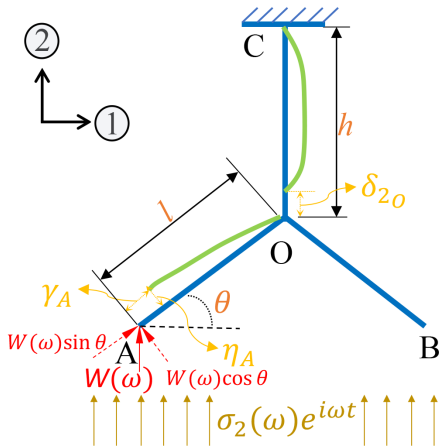
$$
\begin{aligned}
-\delta_2(\omega) = \eta_A(\omega)\cos\theta - \gamma_A(\omega)\sin\theta &= P(\omega)\left(\frac{\sin\theta\cos\theta}{K_{55}(\omega)} - \frac{\sin\theta\cos\theta}{K_{66}(\omega)}\right) \\
&= \frac{P(\omega)\sin\theta\cos\theta}{K_{55}(\omega)}\left(1 - \frac{K_{55}(\omega)}{K_{66}(\omega)}\right) \quad (31)
\end{aligned}
$$

- The total strain in the 2-direction is

$$
-\epsilon_2(\omega) = \frac{\delta_2(\omega)}{h + l\sin\theta} = \frac{\sigma_1(\omega)b\sin\theta\cos\theta}{K_{55}(\omega)}\left(1 - \frac{K_{55}(\omega)}{K_{66}(\omega)}\right) \quad (32)
$$

- Using the expressions of the strains in directions 1 and 2 given by Eqs. (29) and (32), we obtain the Poisson's ratio ν_{12}

$$
\nu_{12}(\omega) = -\frac{\epsilon_2(\omega)}{\epsilon_1(\omega)} = \frac{\cos^2\theta\left(1 - \frac{K_{55}(\omega)}{K_{66}(\omega)}\right)}{(h/l + \sin\theta)\sin\theta\left(1 + \cot^2\theta\frac{K_{55}(\omega)}{K_{66}(\omega)}\right)} \quad (33)
$$

- Dynamic equilibrium and deformation patterns of the unit cell under application of a harmonic stress field $\bar{\sigma}_2 = \sigma_2(\omega)e^{i\omega t}$ applied in the 2-direction. This configuration is used for the derivation of the transverse Young's modulus $E_2(\omega)$ and the Poisson's ratio $\nu_{21}(\omega)$.

- For deriving the expression of transverse Young's modulus and Poisson's ratio ν_{21}, a uniform harmonic stress $\bar{\sigma}_2 = \sigma_2(\omega)e^{i\omega t}$ is applied to the unit cell in direction-2.
- From the free-body diagram depicting the dynamic equilibrium at the steady state condition, we deduce that the the deformation of the unit cell is symmetric about the OC line.
- It addition, the point O has no deflection in the 1-direction. Therefore, it is sufficient to consider the deflection of point A or B with respect to point C under the applied stress.
- Considering point A, the harmonic stress results in a harmonic vertical force $\bar{W} = W(\omega)e^{i\omega t}$ for a given frequency ω. The amplitude of this vertical force is given by

$$W(\omega) = \sigma_2(\omega)bl\cos\theta \tag{34}$$

- Considering η_A and γ_A as deformations transverse and along the inclined member AO, we have

$$\eta_A(\omega) = \frac{W(\omega)\cos\theta}{K_{55}(\omega)} \quad \text{and} \quad \gamma_A(\omega) = \frac{W(\omega)\sin\theta}{K_{66}(\omega)} \tag{35}$$

Here K_{55} and K_{66} are elements of the stiffness matrix of the member AO.

- The deflection in the 2-direction is therefore

$$
\begin{aligned}
\delta_{2_{\mathrm{AO}}}(\omega) &= \eta_A(\omega)\cos\theta + \gamma_A(\omega)\sin\theta = W(\omega)\left(\frac{\cos^2\theta}{K_{55}(\omega)} + \frac{\sin^2\theta}{K_{66}(\omega)}\right) \\
&= \frac{W(\omega)\cos^2\theta}{K_{55}(\omega)}\left(1 + \tan^2\theta\frac{K_{55}(\omega)}{K_{66}(\omega)}\right)
\end{aligned}
\tag{36}
$$

- The total force acting in the 2-direction at point O is $2W$. Therefore, the displacement of point O in the 2-direction arising from the axial deformation of the vertical member OC is

$$
\delta_{2_{\mathrm{O}}}(\omega) = \frac{2W(\omega)}{K_{66}^{(h)}(\omega)}
\tag{37}
$$

- Here $(\bullet)^{(h)}$ corresponds to the properties arising from the vertical member OC of length h. The total deflection in the 2-direction is therefore

$$
\delta_2(\omega) = \delta_{2_{\mathrm{AO}}}(\omega) + \delta_{2_{\mathrm{O}}}(\omega) = \frac{W(\omega)\cos^2\theta}{K_{55}(\omega)}\left(1 + \tan^2\theta\frac{K_{55}(\omega)}{K_{66}(\omega)} + 2\sec^2\theta\frac{K_{55}(\omega)}{K_{66}^{(h)}(\omega)}\right)
\tag{38}
$$

- The strain the 2-direction is obtained as

$$\epsilon_2(\omega) = \frac{\delta_2(\omega)}{h + l\sin\theta} = \frac{\sigma_2(\omega)b\cos^3\theta}{K_{55}(\omega)(h/l + \sin\theta)}\left(1 + \tan^2\theta\frac{K_{55}(\omega)}{K_{66}(\omega)} + 2\sec^2\theta\frac{K_{55}(\omega)}{K_{66}^{(h)}(\omega)}\right)$$
(39)

- Using this, the Young's modulus in 1-direction is obtained in terms of the elements of the stiffness matrix as

$$E_2(\omega) = \frac{\sigma_2(\omega)}{\epsilon_2(\omega)} = \frac{K_{55}(\omega)(h/l + \sin\theta)}{b\cos^3\theta\left(1 + \tan^2\theta\frac{K_{55}(\omega)}{K_{66}(\omega)} + 2\sec^2\theta\frac{K_{55}(\omega)}{K_{66}^{(h)}(\omega)}\right)}$$
(40)

- To obtain the Poisson's ratio ν_{21}, we need to obtain the strain in the direction 1 due to the applied stress in the 2-direction as

$$\delta_1(\omega) = \gamma_A(\omega)\cos\theta - \eta_A(\omega)\sin\theta = -W(\omega)\left(\frac{\sin\theta\cos\theta}{K_{55}(\omega)} - \frac{\sin\theta\cos\theta}{K_{66}(\omega)}\right)$$

$$= -\frac{W(\omega)\sin\theta\cos\theta}{K_{55}(\omega)}\left(1 - \frac{K_{55}(\omega)}{K_{66}(\omega)}\right)$$

(41)

The total strain in the 1-direction is

$$\epsilon_1(\omega) = \frac{\delta_1(\omega)}{l\cos\theta} = -\frac{\sigma_2(\omega)b\sin\theta}{lK_{55}(\omega)}\left(1 - \frac{K_{55}(\omega)}{K_{66}(\omega)}\right)$$

(42)

Using the expressions of the strains in directions 1 and 2 given by Eqs. (29) and (32), we obtain the Poisson's ratio ν_{21}

$$\nu_{21}(\omega) = -\frac{\epsilon_1(\omega)}{\epsilon_2(\omega)} = \frac{(h/l + \sin\theta)\sin\theta\left(1 - \frac{K_{55}(\omega)}{K_{66}(\omega)}\right)}{\cos^2\theta\left(1 + \tan^2\theta\frac{K_{55}(\omega)}{K_{66}(\omega)} + 2\sec^2\theta\frac{K_{55}(\omega)}{K_{66}^{(h)}(\omega)}\right)}$$

(43)

Summary of the results so far

- From equations (30) and (33), it can be observed that only two coefficients of the 6×6 element stiffness matrix of the inclined member, namely, $K_{55}(\omega)$ and $K_{66}(\omega)$, contribute towards the value of E_1 and ν_{12}, which In general are complex valued functions of the frequency ω due to the presence of damping.

- From equations (40) and (33), it can be observed that only two coefficients of the 6×6 element stiffness matrix of the inclined member and one coefficients of the 6×6 element stiffness matrix of vertical member, namely, $K_{55}(\omega)$, $K_{66}(\omega)$ and $K_{66}^{(h)}(\omega)$, contribute towards the value of E_2 and ν_{21}.

- The proposed expressions of the general frequency dependent elastic moduli also conform the reciprocal theorem

$$E_1(\omega)\nu_{21}(\omega) = E_2(\omega)\nu_{12}(\omega) =$$

$$\frac{K_{55}(\omega)}{b\sin\theta \left(1 + \cot^2\theta \frac{K_{55}(\omega)}{K_{66}(\omega)}\right)} \frac{\left(1 - \frac{K_{55}(\omega)}{K_{66}(\omega)}\right)}{\cos\theta \left(1 + \tan^2\theta \frac{K_{55}(\omega)}{K_{66}(\omega)} + 2\sec^2\theta \frac{K_{55}(\omega)}{K_{66}^{(h)}(\omega)}\right)} \quad (44)$$

Shear modulus G_{21}
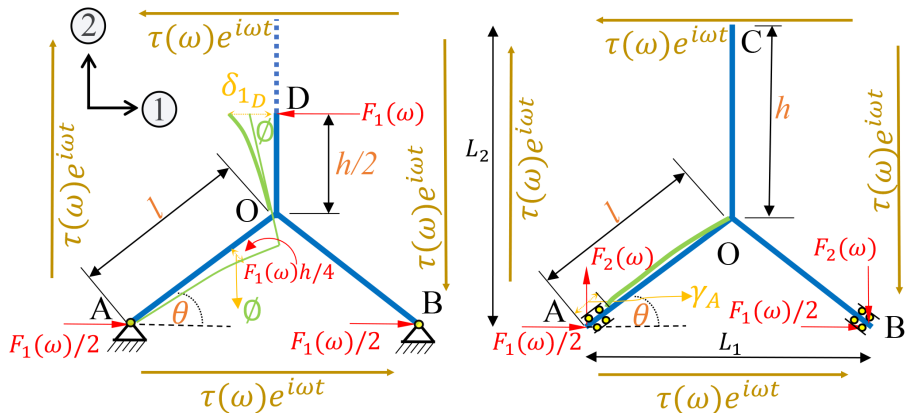
- Dynamic equilibrium and patterns patters of the unit cell under the application of the harmonic shear stress field $\bar{\tau} = \tau(\omega)e^{i\omega t}$. Shear strain due to bending and axial deformation are shown.

- Following a procedure similar to what outlined before, we obtain

$$G_{12}(\omega) = \frac{(h/l + \sin\theta)}{b\cos\theta} \frac{1}{\left(-\frac{h^2}{2lK_{65}(\omega)} + \frac{4K_{66}^{(h/2)}(\omega)}{\left(K_{55}^{(h/2)}(\omega)K_{66}^{(h/2)}(\omega) - \left(K_{56}^{(h/2)}(\omega)\right)^2\right)} + \frac{(\cos\theta + (h/l + \sin\theta)\tan\theta)^2}{K_{66}(\omega)}\right)} \tag{45}$$

- We observed that in total five elements of two different stiffness matrices contribute to the shear modulus. They include two coefficients of the 6×6 element stiffness matrix of the inclined member, namely, $K_{65}(\omega)$, $K_{66}(\omega)$. Additionally three elements of the stiffness matrix of the vertical member with half the length, namely, $K_{55}^{(h/2)}(\omega)$, $K_{56}^{(h/2)}(\omega)$ and $K_{66}^{(h/2)}(\omega)$ contribute to the shear modulus. Like the Youngs moduli, in general the shear modulus is a complex valued function of the frequency ω due to the presence of damping.

- We introduce geometric non-dimensional ratios α and β as

$$\alpha = \frac{t}{l} \tag{46}$$

$$\text{and} \quad \beta = \frac{h}{l} \tag{47}$$

- The moment of inertia and the cross-sectional area are given by

$$I = \frac{1}{12}bt^3 \tag{48}$$

$$\text{and} \quad A = bt \tag{49}$$

- The frequency parameter corresponding to the bending vibration ω_0 is given by

$$\omega_0 = \frac{1}{l^2}\sqrt{\frac{EI}{\rho A}} = \frac{\alpha}{2l}\sqrt{\frac{E}{3\rho}} \tag{50}$$

- The stiffness coefficients are given by

$$K_{55}(\omega) = \frac{\bar{E}Ik_b^3}{l^3}\left(cS + sC\right)/\delta = \bar{E}b\alpha^3 \underbrace{\frac{1}{12}k_b^3\left(cS + sC\right)/\delta}_{\Gamma_1(\omega)}$$

$$K_{66}(\omega) = a_1 = \frac{\bar{E}A}{l}k_a\cot(k_a) = \bar{E}b\alpha\underbrace{k_a\cot(k_a)}_{\Gamma_2(\omega)}$$

$$\text{and}\quad K_{66}^{(h)}(\omega) = \frac{\bar{E}A}{h}k_a^{(h)}\cot(k_a^{(h)}) = \frac{\bar{E}b\alpha}{\beta}k_a^{(h)}\cot(k_a^{(h)}) = \frac{\bar{E}b\alpha}{\beta}\underbrace{\beta k_a\cot\beta k_a}_{\Gamma_3(\omega)}$$

$$(51)$$

- In the above equations we have

$$\bar{E} = E(1 + i\omega c_k)$$

$$k_b^4 = \frac{\rho A\omega^2 L^4\left(1 - ic_m/\omega\right)}{\bar{E}I} = \frac{\omega^2}{\omega_0^2}\frac{\left(1 - ic_m/\omega\right)}{\left(1 + i\omega c_k\right)} \qquad (52)$$

$$k_a^2 = \frac{\alpha^2}{12}k_b^4 \quad\text{and}\quad k_a^{(h)^2} = \beta^2 k_a^2$$

- Upon some algebraic simplifications, we obtain the closed-form expressions

$$E_1(\omega) = \frac{\bar{E}\alpha^3 k_b^3 \left(sC + cS\right)\cos\theta}{\left(\beta + \sin\theta\right)\left(12\delta\sin^2\theta + \alpha^2\cos^2\theta \frac{k_b^3(sC+cS)}{k_a\cot k_a}\right)} \tag{53}$$

$$E_2(\omega) = \frac{\bar{E}\alpha^3 k_b^3 \left(sC + cS\right)\left(\beta + \sin\theta\right)}{12\delta\cos^3\theta + \alpha^2(\sin^2\theta + 2\cot k_a/\cot\beta k_a)\cos\theta \frac{k_b^3(sC+cS)}{k_a\cot k_a}} \tag{54}$$

$$\nu_{12}(\omega) = \frac{\cos^2\theta \left(12\delta k_a\cot k_a - \alpha^2 k_b^3\left(sC + cS\right)\right)}{\left(\beta + \sin\theta\right)\sin\theta \left(12\delta k_a\cot k_a + \alpha^2 k_b^3\left(sC + cS\right)\cot^2\theta\right)} \tag{55}$$

$$\nu_{21}(\omega) = \frac{\left(\beta + \sin\theta\right)\sin\theta \left(12\delta k_a\cot k_a - \alpha^2 k_b^3\left(sC + cS\right)\right)}{12\delta\cos^2\theta + \alpha^2(\sin^2\theta + 2\cot k_a/\cot\beta k_a)\frac{k_b^3(sC+cS)}{k_a\cot k_a}} \tag{56}$$

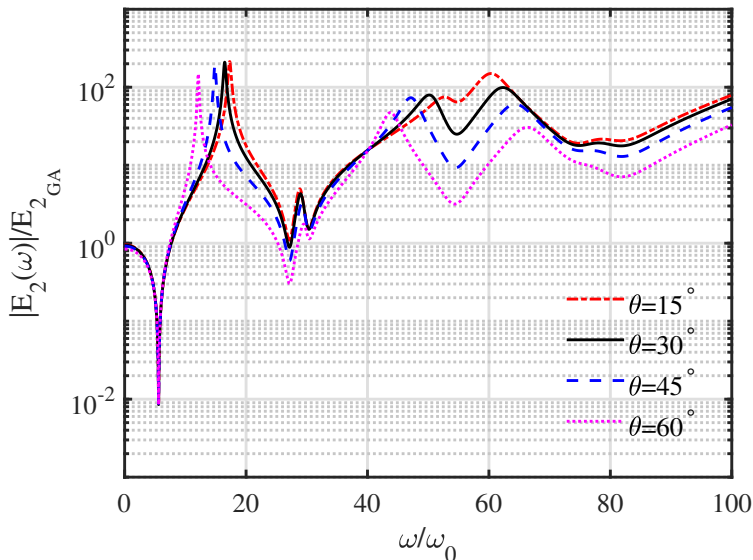Here the frequency-dependent complex quantities are given by

$$\delta = 1 - cC$$
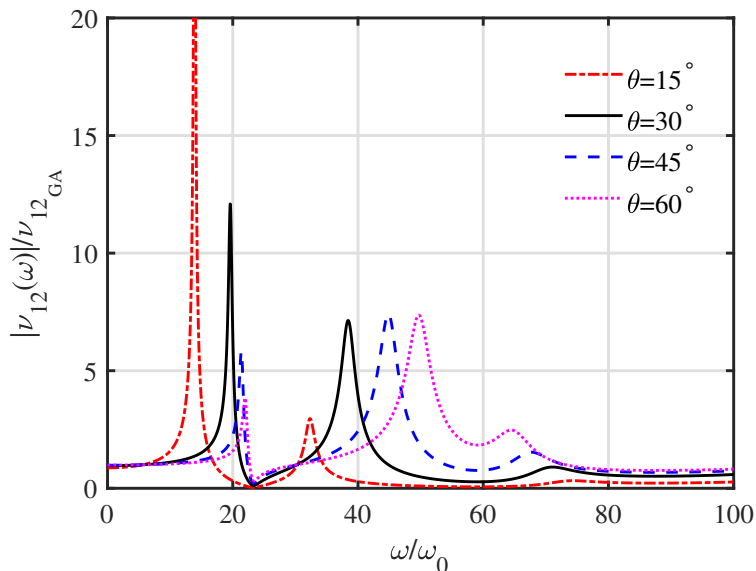$$\text{and} \quad s = \sin k_b, \quad c = \cos k_b, \quad S = \sinh k_b, \quad C = \cosh k_b \tag{57}$$
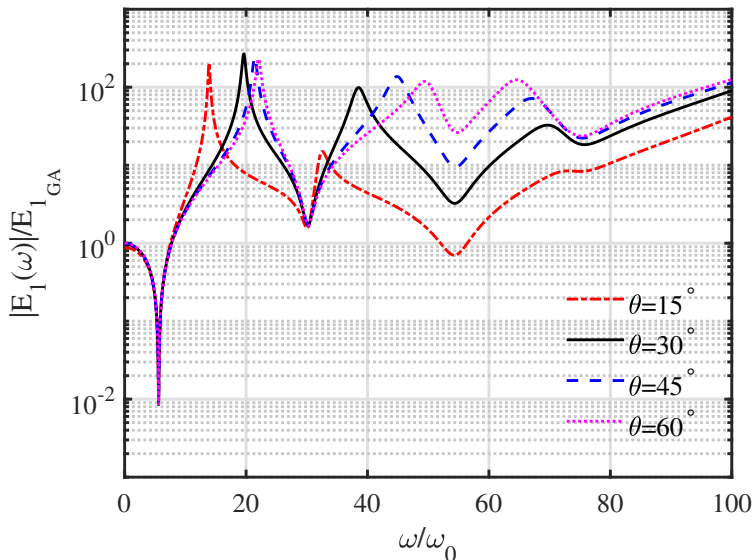
- $\alpha = t/l = 0.1$, $\beta = h/l = 2$, $c_m = 10^{-2}$, $c_k = 10^{-5}$ and $\omega_0 = \frac{\alpha}{2l}\sqrt{\frac{E}{3\rho}}$ (values normalised with corresponding classical static values).
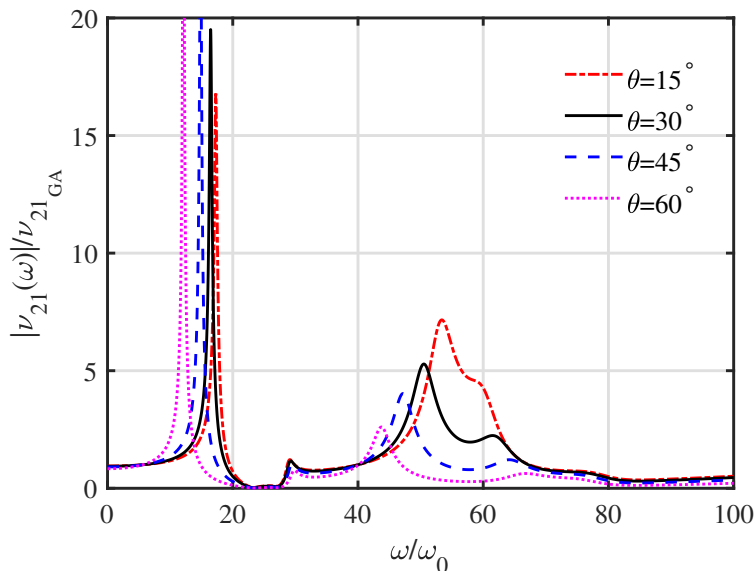
- $\alpha = t/l = 0.1$, $\beta = h/l = 2$ and the damping constants are $c_m = 10^{-2}$ and $c_k = 10^{-5}$ (values normalised with corresponding classical static values).

- $\alpha = t/l = 0.1$, $\beta = h/l = 2$ and the damping constants are $c_m = 10^{-2}$ and $c_k = 10^{-5}$ (values normalised with corresponding classical static values).

- $\alpha = t/l = 0.1$, $\beta = h/l = 2$ and the damping constants are $c_m = 10^{-2}$ and $c_k = 10^{-5}$ (values normalised with corresponding classical static values).

- For analytical simplification, we consider the elemental beams are axially rigid.
- For this case, the Poisson's ratio reduces to the classical case and they don't change with respect to frequency.
- Simplified elastic moduli become:

Simplified $E_1(\omega)$

$$
\begin{aligned}
E_1(\omega) &= \frac{K_{55}(\omega)l\cos\theta}{(h + l\sin\theta)\bar{b}\sin^2\theta} \\
&= \frac{Et^3 l\cos\theta b^3(\cos(bl)\sinh(bl) + \cosh(bl)\sin(bl))}{12(h + l\sin\theta)\sin^2\theta(1 - \cos(bl)\cosh(bl))}
\end{aligned}
\tag{58}
$$

where

$$
b^4 = \frac{m\omega^2(1 - \mathrm{i}\zeta_m/\omega)}{EI(1 + \mathrm{i}\omega\zeta_k)}
\tag{59}
$$

Simplified $E_2(\omega)$

$$
\begin{aligned}
E_2(\omega) &= \frac{K_{55}(\omega)(h + l\sin\theta)}{l\bar{b}\cos^3\theta} \\
&= \frac{Et^3(h + l\sin\theta)b^3\left(\cos(bl)\sinh(bl) + \cosh(bl)\sin(bl)\right)}{12l\cos^3\theta(1 - \cos(bl)\cosh(bl))}
\end{aligned}
\tag{60}
$$

Simplified $G_{12}(\omega)$

$$
\begin{aligned}
G_{12}(\omega) &= \frac{(h + l\sin\theta)}{2l\bar{b}\cos\theta}\frac{1}{\left(-\frac{h^2}{4lD_{65}^s} + \frac{2}{\left(D_{55}^v - \frac{(D_{56}^v)^2}{D_{66}^v}\right)}\right)} \\
&= \frac{Et^3(h + l\sin\theta)b^3\sin(bl)\sinh(bl)\left(1 + \cos(bh/2)\cosh(bh/2)\right)}{6l\cos\theta\left[h^2b\left(1 - \cos(bl)\cosh(bl)\right)\left(1 + \cos(bh/2)\cosh(bh/2)\right)\right.} \\
&\quad \left. + 8l\sin(bl)\sinh(bl)\left(\cosh(bh/2)\sin(bh/2) - \sinh(bh/2)\cos(bh/2)\right)\right]
\end{aligned}
\tag{61}
$$

- Considering the static case, that is, when the the frequency $\omega \to 0$, we have

$$\lim_{\omega \to 0} K_{55}(\omega) = 12 \frac{EI}{l^3} = 12 \left(\frac{1}{12} E \bar{b} t^3 \right) \frac{1}{l^3} = E \bar{b} \left(\frac{t}{l} \right)^3 \qquad (62)$$

- Substituting this in the expressions of $E_1(\omega)$ and $E_2(\omega)$ in equations (58) and (60) we have

$$\lim_{\omega \to 0} E_1(\omega) = \frac{l \cos \theta}{(h + l \sin \theta) \bar{b} \sin^2 \theta} \lim_{\omega \to 0} K_{55}(\omega) \qquad (63)$$

$$= E \left(\frac{t}{l} \right)^3 \frac{l \cos \theta}{(h + l \sin \theta) \sin^2 \theta}$$

$$\text{and} \quad \lim_{\omega \to 0} E_2(\omega) = \frac{(h + l \sin \theta)}{l \bar{b} \cos^3 \theta} \lim_{\omega \to 0} K_{55}(\omega) = E \left(\frac{t}{l} \right)^3 \frac{(h + l \sin \theta)}{l \cos^3 \theta}$$

$$(64)$$

- The above expressions match exactly with the original classical expressions of E_1 and E_2.

- The shear modulus $G_{12}(\omega)$ given in (61) is a function of four dynamic stiffness coefficients. In the limiting case they become

$$\lim_{\omega \to 0} D_{65}^s = -6\frac{EI}{l^2}, \lim_{\omega \to 0} D_{55}^v = 96\frac{EI}{h^3}, \lim_{\omega \to 0} D_{56}^v = -24\frac{EI}{h^2}, \lim_{\omega \to 0} D_{66}^v = 8\frac{EI}{h} \tag{65}$$

- Substituting these in (61) we have

$$\lim_{\omega \to 0} G_{12}(\omega) = \frac{(h + l\sin\theta)}{2l\bar{b}\cos\theta} \lim_{\omega \to 0} \frac{1}{\left(-\frac{h^2}{4lD_{65}^s} + \frac{2}{\left(D_{55}^v - \frac{(D_{56}^v)^2}{D_{66}^v}\right)}\right)} \tag{66}$$

$$= \frac{(h + l\sin\theta)}{2l\bar{b}\cos\theta} \frac{1}{(1/24)\frac{h^2 l}{EI} + (1/12)\frac{h^3}{EI}} = E\left(\frac{t}{l}\right)^3 \frac{\left(\frac{h}{l} + \sin\theta\right)}{\left(\frac{h}{l}\right)^2 \left(1 + 2\frac{h}{l}\right)\cos\theta}$$

- This shows that the shear modulus $G_{12}(\omega)$ also reduces to the classical equation in the static limit.
- These expressions should be viewed as the dynamic generalisation of the conventional equivalent elastic moduli of the hexagonal cellular material.

- The expressions of E_1 and E_2 are proportional to $K_{55}(\omega)$, which is a complex frequency-dependent coefficient. Therefore, we study it's behaviour in the undamped limit to understand the the real part of E_1 and E_2.
- Assuming no damping in the system, the parameter b in equation (59) becomes

$$b^4 = \frac{m\omega^2}{EI} \tag{67}$$

- Substituting this in the expression of $K_{55}(\omega)$ and expanding the expression by a Taylor series in the frequency parameter ω we have

$$K_{55}(\omega) = 12\,\frac{EI}{l^3} - \frac{13}{35}\,m\,l\omega^2 - \frac{59}{161700}\,\frac{l^5 m^2 \omega^4}{EI} - \frac{551}{794593800}\,\frac{l^9 m^3 \omega^6}{EI^2} + \cdots \tag{68}$$

- Note that coefficients of some higher order terms of ω are negative. We observe that $K_{55}(\omega)$ appears as a multiplicative term in the expressions of $E_1(\omega)$ and $E_2(\omega)$ in equations (58) and (60) and the other terms are positive.
- Therefore, near the vicinity of $\omega \approx 0$, there exist some frequency beyond which the effective elastic moduli of honeycomb will be negative.

- Retaining up to terms of order ω^4 in equation (69), the critical value of ω can be obtained by setting $K_{55}(\omega) = 0$ as

Negative E_1, E_2

$$K_{55}(\omega) \approx 12\,\frac{EI}{l^3} - \frac{13}{35}\,m\,l\omega^2 - \frac{59}{161700}\,\frac{l^5 m^2 \omega^4}{EI} = 0$$

$$\text{or} \quad \omega^*_{E_1, E_2} = 5.598\,\frac{1}{l^2}\sqrt{\frac{EI}{m}}$$

(69)

- For lightly damped systems, beyond this frequency value, the equivalent Young's moduli E_1 and E_2 will be negative.
- Since the discovery of the Young's modulus over three centuries ago, it has been generally recognised as a positive quantity. When a dynamic equilibrium is considered, our results show that fore cellular metamaterials the Young's moduli can be negative, contradicting notions established for centuries.
- Similar observation has been made in the context of acoustics metamaterials with sub-wavelength scale oscillators.

- For the shear modulus, it is also possible to expand the frequency dependent expression (61) to expand in a Taylor series in ω about $\omega = 0$ as

$$G_{12}(\omega) = \frac{(h + l\sin\theta)}{2l\bar{b}\cos\theta}\left[24\frac{EI}{h^2(2h+l)} - \frac{11}{420}\frac{m(9h^5+8l^5)\omega^2}{h^2(2h+l)^2}\right.$$
$$-\frac{1}{46569600}\frac{m^2(55461h^9l - 191664h^5l^5 + 198912l^9h + 3111h^{10} + 14272l^{10})\omega^4}{EIh^2(2h+l)^3}\cdots$$

(70)

- Considering only up to the second-order terms, we obtain the following fundamental inequality regarding the frequency for negative value of G_{12}

Negative G_{12}

$$\frac{120}{\sqrt{160 + 75(h/l)^4}}\frac{1}{l^2}\sqrt{\frac{EI}{m}} < \omega_{G_{12}}^* < 30.2715\sqrt{\frac{1 + 2(h/l)}{8 + 9(h/l)^5}}\frac{1}{l^2}\sqrt{\frac{EI}{m}}$$
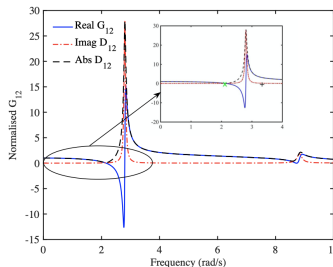
(71)

- Unlike the equivalent expression for the Young's moduli E_1 and E_2 in (69), for the minimum frequency above which G_{12} becomes negative depends on the h/l ratio.
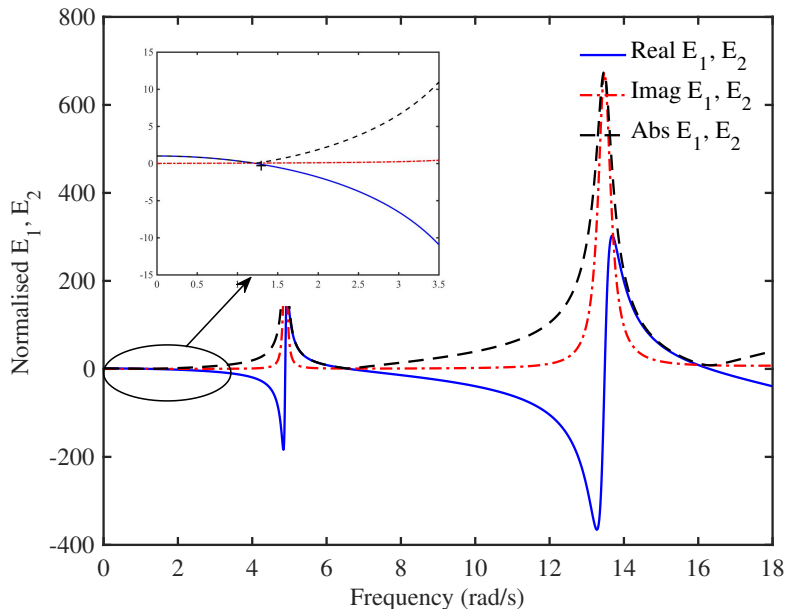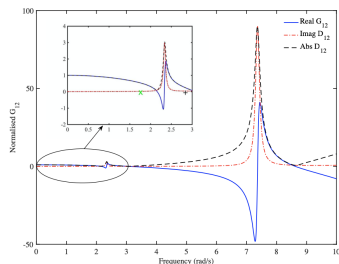
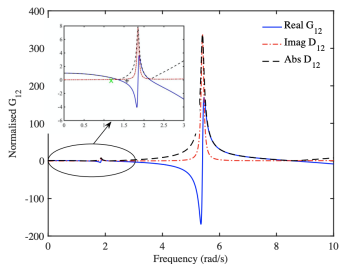The real and imaginary parts and the amplitude of the normalised value of E_1 and E_2 as a function of frequency

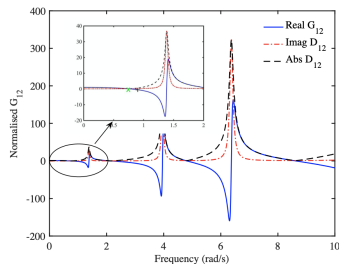(a) $h/l = 0.5$, $2.0430 < \omega_{G_{12}}^* < 3.2502$
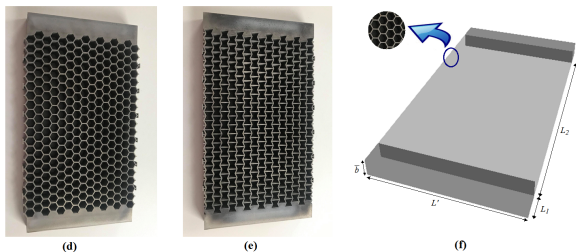
(b) $h/l = 1.0$, $1.7103 < \omega_{G_{12}}^* < 2.7783$
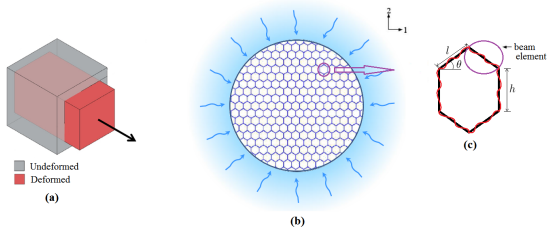
(c) $h/l = 1.5$, $1.1286 < \omega_{G_{12}}^* < 1.5139$

(d) $h/l = 2.0$, $0.71090 < \omega_{G_{12}}^* < 0.8596$

The real and imaginary parts and the amplitude of the normalised value of G_{12} as a function of frequency for four different values of h/l.

Lattice metamaterials under a vibrating environment. (a) Deformed shape of an equivalent continuum under uniaxial static (/quasi-static) deformation (b) Schematic representation of a hexagonal lattice microstructure under dynamic environment (for example, lattice microstructure as part of a larger host structure under wave propagation, vibration etc.).The curved arrows in this figure are symbolic representation of propagating wave. (c) Unit cell under a dynamic environment (d - e) Additively manufactured non-auxetic and auxetic samples of hexagonal lattice structures with intrinsic material as Titanium alloy Ti-6Al-4V (f) Equivalent continuum representation of the test specimen

Additive manufacturing of the honeycomb

- The Ti-6Al-4V lattice materials were additively manufactured on a Renishaw RenAM 500M, which is a Laser Powder Bed Fusion (L-PBF) process. The RenAM 500M system uses a 500W Ytterbium fibre laser to melt Ti-6Al-4V gas atomised powder onto a 250mm $\times$ 250mm build plate, on a layer by layer basis, up to a maximum built height of 280mm.

- In this instance the Ti-6Al-4V powder was ELI grade and supplied by LPW. The parameters used in these builds were a power of 400W, a layer thickness of 60μm, a point distance of 80μm, an exposure time of 60μs, and a hatch spacing of 100μm. Both the non-auxetic lattice in figure 1(d) and the auxetic lattice in figure 1(e) were built directly onto the base plate without any support structure, but with an additional 1mm sacrificial layer.

- The lattices were then removed from the base plate using Electric Discharge Machining (EDM) so that the thickness was 15mm.

- The final dimension of the lattices in XY plane come to 215 mm $\times$ 115 mm. Residual stress is known to affect mechanical properties, however, no stress relieving post-build heat treatments were used in this instance, which resulted in a small spring-back deformation in the build direction after removal from the plate.
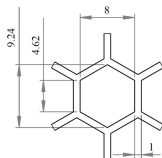
- The additively manufactured honeycomb structure is tested using an impact hammer. This is achieved with the aid of DataPhysics software and the 901 Series dynamic signal analyser to return the Frequency Response Functions (FRFs) between the force sensor in the hammer tip and the accelerometers.

- After some initial testings, a frequency bandwidth of 6400Hz is used for the sample. Due to the higher natural frequencies, a stiff tip is used on the hammer in order to create a shorter pulse duration and increase the frequency range generated, and an exponential window was used to ameliorate the potential problem of leakage and improve the signal to noise ratio by reducing the influence of the noise long after the impact

- To obtain the in-plane axial response, the impact of the hammer is applied to the top of the honeycomb structure, as centrally as can be practically achieved. Using the accelerometers, accelerance (acceleration per unit force) frequency response functions (FRF) are produced. These are evaluated, determining the response to excitation vibration and thus the modal response at resonance. In total five channels of data have been stored. They include four accelerometers and the impact hammer.

- The real and imaginary parts of the frequency response for all the five channels have been stored for all the frequency points. The relative deformation of the lattice is obtained by subtracting the accelerometer reading of the opposite edges and dividing the resulting complex vector by frequency-square (note $A = -\omega^2 X$, where A is the acceleration and X is the displacement).

- The effective dynamic strain is therefore obtained by dividing this quantity by the overall length of the lattice. The measured frequency dependent force is divided by the surface area of the top of the lattice to obtain the applied stress. The ratio of the effective stress and stain calculated this way gives the measured Young's modulus and is plotted in subfigure (c) by separating the real and imaginary parts.
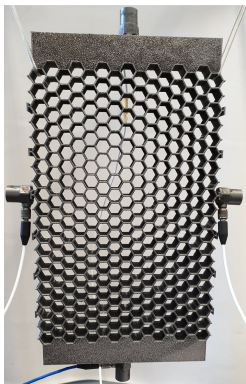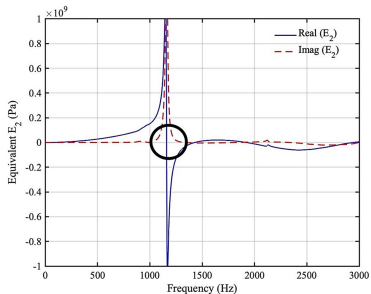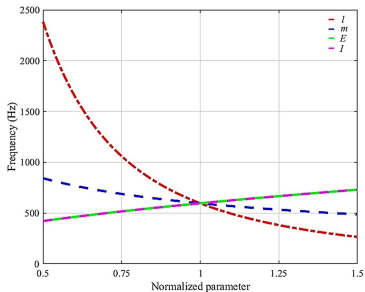
(a)

(b)

(c)

(d)

- **Onset of negative Young's moduli.** (a) Description of the experimental setup
- (b) Dimensions (in c.m.) of a unit cell considered for the experimental investigation
- (c) Experimental results for variation of Young's modulus with frequency (real and imaginary components of E_2 are plotted as a function of frequency)
- (d) Dependence of the onset of negative Young's moduli on microstructural geometry and intrinsic material properties (Here the critical frequency for the onset of negative Young's moduli is plotted as a function of the geometric and material properties. These parameters are plotted along the abscissa in a normalized form with respect to the respective nominal values considered in the experimental investigations)

- An augmented dynamic stiffness approach based generic analytical framework is presented for analysing the elastic moduli of lattice materials under steady-state vibration conditions.

- Using the principle of dynamic equilibrium on a unit cell with a homogenisation technique, closed-form expressions have been obtained for E_1, E_2, ν_{12}, ν_{21} and G_{12}. These expressions are complex valued and functions of the frequency.

- The new results reduce to classical formulae of Gibson and Ashby for the special case in the static limit.

- Experimental results on 3D printed lattice show the onset of negative effective Young's moduli for the first time.

- Closed-form expressions for the critical frequency leading to negative effective Young's moduli have been derived.

- This analytical framework leading to the development of closed-form expressions for the frequency-dependent elastic moduli provides a computationally efficient and physically insightful approach for investigating the global lattice behaviour under dynamic conditions.

$$E_1(\omega) = \frac{K_{55}(\omega)\cos\theta}{b(h/l+\sin\theta)\sin^2\theta\left(1+\cot^2\theta\frac{K_{55}(\omega)}{K_{66}(\omega)}\right)} \tag{72}$$

$$E_2(\omega) = \frac{K_{55}(\omega)(h/l+\sin\theta)}{b\cos^3\theta\left(1+\tan^2\theta\frac{K_{55}(\omega)}{K_{66}(\omega)}+2\sec^2\theta\frac{K_{55}(\omega)}{K_{66}^{(h)}(\omega)}\right)} \tag{73}$$

$$\nu_{12}(\omega) = \frac{\cos^2\theta\left(1-\frac{K_{55}(\omega)}{K_{66}(\omega)}\right)}{(h/l+\sin\theta)\sin\theta\left(1+\cot^2\theta\frac{K_{55}(\omega)}{K_{66}(\omega)}\right)} \tag{74}$$

$$\nu_{21}(\omega) = \frac{(h/l+\sin\theta)\sin\theta\left(1-\frac{K_{55}(\omega)}{K_{66}(\omega)}\right)}{\cos^2\theta\left(1+\tan^2\theta\frac{K_{55}(\omega)}{K_{66}(\omega)}+2\sec^2\theta\frac{K_{55}(\omega)}{K_{66}^{(h)}(\omega)}\right)} \tag{75}$$

$$G_{12}(\omega) = \frac{(h/l+\sin\theta)}{b\cos\theta}$$
$$\frac{1}{\left(-\frac{h^2}{2lK_{65}(\omega)}+\frac{4K_{66}^{(h/2)}(\omega)}{\left(K_{55}^{(h/2)}(\omega)K_{66}^{(h/2)}(\omega)-\left(K_{56}^{(h/2)}(\omega)\right)^2\right)}+\frac{(\cos\theta+(h/l+\sin\theta)\tan\theta)^2}{K_{66}(\omega)}\right)} \tag{76}$$

Some of our papers on this topic

1. Cajic, M., Karlicic, D., Paunovic, S. and Adhikari, S., "A fractional calculus approach to metadamping in phononic crystals and acoustic metamaterials", Theoretical and Applied Mechanics, 47[1] (2020), pp. 81-97.

2. Adhikari, S., Mukhopadhyay, T., Shaw, A. and Lavery, N. P., "Apparent negative values of Young's moduli of lattice materials under dynamic conditions", International Journal of Engineering Science, 150[5] (2020), pp. 103231.

3. Chandra, Y., Saavedra Flores. E. I. and Adhikari, S., "Buckling of 2D nano hetero structures with moire patterns", Computational Materials Science, 177[5] (2020), pp. 109507.

4. Chandra, Y., Mukhopadhyay, T., Adhikari, S., and Figiel, L., "Size-dependent dynamic characteristics of graphene based multi-layer nano hetero-structures", Nanotechnology, 31[14] (2020), pp. 145705.

5. Mukhopadhyay, T., Adhikari, S., and Alu, A., "Theoretical limits for negative elastic moduli in subacoustic lattice materials", Physical Review B, Vol. 99, 2019, pp. 094108.

6. Mukhopadhyay, T., Adhikari, S., and Alu, A., "Probing the frequency-dependent elastic moduli of lattice materials", Acta Materialia, Vol. 165, No. 2, 2019, pp. 654-665.

7. Mukhopadhyay, T., Adhikari, S., and Batou, A., "Viscoelastic mechanical properties of irregular quasi-periodic lattices with spatially correlated material and structural attributes", International Journal of Mechanical Science, Vol. 150, No. 1, 2019, pp. 784-806.

8. Mukhopadhyay, T., Mahata, T., Adhikari, S., and Zaeem, M. A., "Probing the shear modulus of two-dimensional multiplanar nanostructures and heterostructures", Nanoscale, Vol. 10, No. 11, 2018, pp. 5280-5294.

9. Mukhopadhyay, T., Mahata, A., Adhikari, S. and Asle Zaeem, M., "Effective mechanical properties of multilayer nano-heterostructures", Nature Scientific Reports, (2017), pp. 15818:1-13.

10. Mukhopadhyay, T. and Adhikari, S., "Effective in-plane elastic properties of quasi-random spatially irregular hexagonal lattices", International Journal of Engineering Science 119 (2017), pp. 142-179.

11. Mukhopadhyay, T., Mahata, A., Asle Zaeem, M. and Adhikari, S., "Effective elastic properties of two dimensional multiplanar hexagonal nano-structures", 2D Materials, 4[2] (2017), pp. 025006:1-15.

12. Mukhopadhyay, T. and Adhikari, S., "Stochastic mechanics of metamaterials", Composite Structures, 162[2] (2017), pp. 85-97.

13. Mukhopadhyay, T. and Adhikari, S., "Free vibration of sandwich panels with randomly irregular honeycomb core", ASCE Journal of Engineering Mechanics,141[6] (2016), pp. 06016008:1-5.

14. Mukhopadhyay, T. and Adhikari, S., "Equivalent in-plane elastic properties of irregular honeycombs: An analytical approach", International Journal of Solids and Structures, 91[8] (2016), pp. 169-184.

15. Mukhopadhyay, T. and Adhikari, S., "Effective in-plane elastic properties of auxetic honeycombs with spatial irregularity", Mechanics of Materials, 95[2] (2016), pp. 204-222.